From subduction to collision: Control of deep processes on the evolution of convergent plate boundary

Vincent Regard, Claudio Faccenna, Joseph Martinod, Olivier Bellier, Jean-Charles Thomas

From subduction to collision: Control of deep processes on the evolution of convergent plate boundary

Vincent Regard,[1] Claudio Faccenna,[2] Joseph Martinod,[3,4] Olivier Bellier,[1] and Jean-Charles Thomas[5]

Received 25 April 2002; revised 2 December 2002; accepted 30 January 2003; published 19 April 2003.

[1] Using laboratory experiments, we investigate the dynamics of the collisional process that follows the closure of an oceanic basin. The evolution of these experiments systematically shows four successive episodes of deformation, which correspond to (1) the initiation of oceanic subduction, (2) a mature period of oceanic subduction, (3) an episode of continental subduction, during which the trench absorbs all the convergence and the superficial tectonic regime does not change significantly within the continental plates, and (4) continental collision that starts when the trench locks and convergence is absorbed by a system of thrust faults and folds. We observe that the amount of continental material that subducts before the onset of collision depends on the slab pull exerted by the subducted oceanic lithosphere. The slab-pull force, in turn, depends on the amount of subducted oceanic material, on the thickness of the convective mantle, and also on the rheology of the slab. Our experiments, indeed, suggest that parts of the oceanic slab may separate from the superficial slab to sink rapidly in the mantle, decreasing the slab-pull level and triggering the rapid onset of collision. We observe two possible modes of slab deformation: slab break-off and development of viscous instabilities. We define two dimensionless rheological numbers to characterize the possible occurrence of these modes of deformation. In all cases, oceanic closure is followed by episode of continental subduction during which the continental lithosphere may reach depths varying between 50 and 450 km, prior to the onset of continental collision. *INDEX TERMS:* 0905 Exploration Geophysics: Continental structures (8109, 8110); 8102 Tectonophysics: Continental contractional orogenic belts; 8110 Tectonophysics: Continental tectonics—general (0905); 8150 Tectonophysics: Plate boundary—general (3040); *KEYWORDS:* subduction, collision, continental subduction, oceanic closure, analog experiments

Citation: Regard, V., C. Faccenna, J. Martinod, O. Bellier, and J.-C. Thomas, From subduction to collision: Control of deep processes on the evolution of convergent plate boundary, *J. Geophys. Res.*, *108*(B4), 2208, doi:10.1029/2002JB001943, 2003.

1. Introduction

[2] The collisional process is generally considered as the result of the docking of continental plates after the closure of an oceanic basin. However, several orders of evidence indicate that arrival at the trench of a continental margin does not produce either trench locking or the formation of mountain belts.

[3] The total shortening between India and Eurasia has been estimated to between 2600 ± 900 km [*Patriat and Achache*, 1984]. A large part of this shortening, about 1000 km, should have been accommodated by subduction of the Indian continental lithosphere beneath Eurasia [*Matte et al.*, 1997], as confirmed by tomographic results [*van der Voo et al.*, 1999a, 1999b]. Similar, though less spectacular, examples of continental subduction have been described in other colliding regions such as in the Alps, in the northern Apennines, in Arabia, corroborating the idea that continental lithosphere, or part of it, can subduct to great depth. The finding of ultrahigh-pressure metamorphic minerals such as coesite on metasediments deposited on continental margins reinforces this idea indicating that these rocks suffered pressures of about 30–35 kbar [*Chopin*, 1984; *Smith*, 1984; *Caby*, 1994; *Wain*, 1997; *Ernst and Liou*, 2000; *Katayama et al.*, 2000; *Liou et al.*, 2000].

[4] Buoyancy analysis indicates that only a continental crust thicker than 15 km makes the lithosphere positively buoyant [*Cloos*, 1993]. When a 35-km-thick continental crust enters at trench following the subduction of an oceanic plate, and if the oceanic slab is long enough to reach the 660-km discontinuity, then the continent may subduct to a depth of 100–300 km to compensate the negative buoyancy

[1]Centre Européen de Recheche et d'Enseignement en Géosciences de l'Environnement, UMR CNRS 6635, Université Aix-Marseille III, Aix-en-Provence, France.
[2]Dipartimiento di Scienze Geologiche, Università Roma tre, Rome, Italy.
[3]Institut de Recherche et Développement, Santiago, Chile.
[4]Now at Institut de Recherche et Développement, Laboratoire de Mécanismes de Transfert en Géologie, Toulouse, France.
[5]Laboratoire de Géophysique Interne et Tectonophysique, UMR CNRS 5559, Université Joseph Fourier, Grenoble, France.

0148-0227/03/2002JB001943$09.00

of the oceanic slab [*Ranalli*, 2000; *Ranalli et al.*, 2000]. The amount of continental subduction can considerably increase if external forces push the lithosphere to sink into the mantle, if the crust is scraped off from the mantle of the subducting lithosphere, or if phase transformations are considered.

[5] The delamination of the dense, lithospheric mantle from the crust is, indeed, a suitable mechanism to facilitate continental subduction. This mechanism is often claimed to occur in continental convergence. However, crust-mantle delamination is possible only for the case of a weak (i.e., hot) lower crust rheology [*Ranalli*, 2000]. The possible increase in density of the crust by phase changes, conversely, facilitates continental subduction also in the case of strong crustal rheology, since lower crustal rocks can be eclogitized [*Austrheim*, 1987, 1994; *Le Pichon et al.*, 1992, 1997; *Dewey et al.*, 1993].

[6] Evaluations of the amount of continental subduction based on buoyancy calculations, however, are restricted to the case of undeformed subducting lithosphere. Recent numerical experiments show that a continental slab can deform at depth by partial removal of dense viscous mantle material [*Pysklywec et al.*, 2000] or by break-off of the slab [*Wortel and Spakman*, 2000]. In particular, the removal of viscous mantle material can be approximated to a Rayleigh-Taylor instability, as it is driven by thermal buoyancy and resisted by viscous forces [e.g., *Houseman et al.*, 1981; *Buck and Toksöz*, 1983; *England and Houseman*, 1989; *Lenardic and Kaula*, 1995; *Conrad and Molnar*, 1997; *Houseman and Molnar*, 1997; *Molnar et al.*, 1998; *Neil and Houseman*, 1999; *Pysklywec et al.*, 2000]. Slab break-off, conversely, is thought to occur at the continent-ocean transition and within the shallower portion of the *slab* [*Yoshioka and Wortel*, 1995; *Wong A Ton and Wortel*, 1997; *Wortel and Spakman*, 2000]. Both processes produce a similar effect, as they reduce the negative buoyancy of the subducting system and prevent deep subduction of buoyant continental material.

[7] The interaction of these mechanisms and the interplay of different physical parameters limit our knowledge on the behavior of the continental lithosphere at a subduction zone. The possible subduction of continental lithosphere, in fact, excludes that collision results directly from the arrival at trench of continental material. In this sense, the initiation of collisional processes and of mountain building depends on how the slab deforms at mantle depth and how the mantle reacts over geological timescales.

[8] Here, we investigate using laboratory experiments the dynamics of collisional processes after the closure of an oceanic basin. The initiation of collision and the rise of orogens are then explored in a fully dynamical mantle/slab equilibrium. Our results indicate that the collisional process depends on the way the slab deforms at depth and on the style of mantle convection. We observe that the amount of continental material that can be subducted before the onset of collision increases with the slab-pull force exerted by the oceanic subducted lithosphere. This force, in turn, depends on the rheology of the slab and on the amount of oceanic plate. Our experiments show that portions of the slab can be removed during subduction either by viscous deblobbing or by slab break-off, decreasing the slab-pull force and favoring the rapid onset of collision after continental subduction.

2. Laboratory Experiments

[9] Over the last decade, many laboratory experiments scaled for gravity have been assembled to simulate subduction [see *Kincaid and Olson*, 1987; *Shemenda*, 1992; *Chemenda et al.*, 1995; *Griffiths et al.*, 1995; *Guillou-Frottier et al.*, 1995; *Faccenna et al.*, 1996, 1999; *Becker et al.*, 1999]. Few attempts, however, have been succeeded in modeling continental subduction and collision. For the aim of this paper it is important to recall two sets of experiments. The first one was performed by *Davy and Cobbold* [1991], who simulated with similar materials than those used here, modes of continental collision. The second set was performed by *Chemenda et al.* [1995, 1996, 2000], who modeled the subduction of continental lithosphere using solid hydrocarbons simulating a lithosphere characterized by an elastoplastic rheology. Our model has been designed following the *Davy and Cobbold* [1991] and *Faccenna et al.* [1996] approach, with a slab viscosity 2 orders of magnitude larger than the mantle viscosity. We use a ductile-brittle layering for the lithosphere, permitting its internal deformation when descending into the viscous advecting mantle.

2.1. Materials and Experimental Technique

[10] Following an experimental design adopted by previous authors [e.g., *Davy and Cobbold*, 1988, 1991; *Martinod and Davy*, 1994; *Faccenna et al.*, 1996; *Pubellier and Cobbold*, 1996], we simulate the stratified lithospheric rheological profile [e.g., *Ranalli and Murphy*, 1987] by constructing a brittle-ductile layered model (Figure 1), with sand mixture to model the brittle behavior of the upper crust and silicone putty to model the ductile behavior of the lower crust and mantle lithosphere. The sand-silicone layering rests on honey, which simulates the upper mantle.

[11] We use two different kinds of sand-silicone layers, either lighter or denser than the glucose syrup, to represent continental or oceanic lithospheres, respectively. A sand-silicone plate simulating oceanic lithosphere separates two light continental plates. Continental and oceanic plates differ in thickness, density, and viscosity of the upper silicone layer and in thickness and density of the sand layer (Figure 1 and Table 1). The sand is sieved over the entire model, with the exception of a 1-cm-wide strip located at one continent-oceanic boundary (no sand above the silicone plate) (Figure 2). Shortening imposed in the experiment will thus preferentially localize on this side of the oceanic plate. The lower boundary of the box approximates a high gradient viscosity transition.

[12] Models are constructed inside a rectangular Plexiglas tank (50 cm long and 30 cm wide; Figure 1). The box depth varies from 11 to 19 cm. The lateral walls of the tank are lubricated with wax and the sand layer is removed to reduce friction at plate-walls interfaces. Horizontal shortening is achieved displacing a rigid piston at constant velocity perpendicular to the plate margins. The piston is confined in the upper part of the tank and the glucose syrup is free to move underneath (Figure 1). For convenience we shall refer thereafter to regions of the experiment in terms of geographical directions, the southern boundary corresponding to the piston. A squared grid of passive sand markers enables visualization of the surface deformation. Photo-

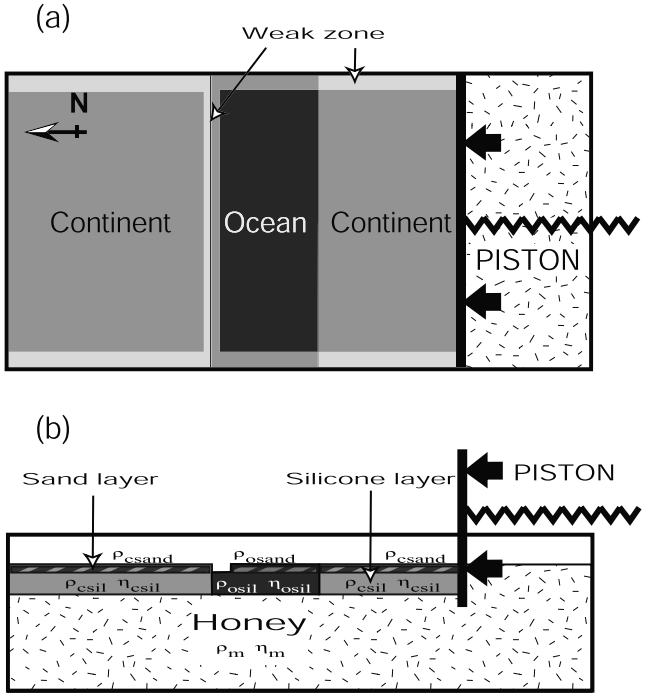

Figure 1. Experimental setup. Sand/silicone plates modeling the lithosphere are lying above honey that represents the upper mantle. These plates are lighter or denser than honey to represent continental or oceanic lithospheres, respectively. The piston is pushing northward at a constant velocity of 4.4 mm h^{-1} scaled to represent 2.3 cm yr^{-1} in nature. The oceanic plate will subduct below the northern continent, the subduction place being determined by the removal of a 1-cm-wide band of sand that weakens the northern margin. Similar weak bands are placed at the lateral boundaries of the box with lateral walls to diminish the boundaries effects.

graphs are taken at regular time intervals in three orientations, top, oblique, and lateral view through the transparent tank walls.

[13] The materials selected to model the stratified oceanic and continental lithosphere have been chosen to fulfill stress similarity criteria scaled for gravity [see *Davy and Cobbold*, 1991]. Material parameters for each experiment and the scaling values are listed in Tables 1 and 2, respectively.

[14] The brittle layer of the lithosphere is modeled using dry sand with uniform grain size mixed with semolina to vary the density from 1250 to 1500 kg m^{-3}. This material obeys to a frictional sliding Mohr-Coulomb criterion (i.e., shear strength linearly increasing with depth) with negligible cohesion and a mean friction angle of about 30° [*Mandl et al.*, 1977]. Therefore it should represent a good analogue for upper crustal rocks [*Byerlee*, 1978; *Davy and Cobbold*, 1991]. In the gravity field ($g_{model} = g_{nature}$), with a length scale factor (L') equal to 1.5×10^{-7} (80 km in nature corresponds to 1.2 cm in the model) and with a density scale factor (ρ') of about 0.5 ($\rho_{model}/\rho_{nature}$ = 1500 kg m^{-3}/3000 kg m^{-3}), we obtain the dimensionless stress scale factor $\sigma' = L' \rho'$. For example, a lithostatic stress level of ~530 MPa at the base of a 18-km-thick oceanic brittle layer scales to a stress level at the base of the sand layer of 32 Pa, with a thickness of 2–3 mm (see Table 2). The stress scale factor is used to determine the rheological layering of the model lithosphere [*Davy and Cobbold*, 1991].

[15] Silicone putty is a nearly Newtonian fluid [*Weijermars and Schmeling*, 1986; *Davy and Cobbold*, 1991]. We use a pure silicone base with iron powder added to increase its density. This material is used to model the layers of the lithosphere in which ductile creep predominates (i.e., lower crust and mantle), with two main restrictions. The first is that viscosity within each layer does not vary with depth (average over the lithospheric depth). Analytical calculations demonstrate that the formation of lithospheric instability is not significantly modified by this approximation [*Martinod and Davy*, 1992]. The second restriction is that silicone putty is a nearly Newtonian material, whereas laboratory data indicate that upper mantle materials obey to creep power law of deformation with a stress exponent ranging between 2 and 5 [e.g., *Brace and Kohlstedt*, 1980]. We choose the viscosity of silicone and the experimental strain rate to scale the strength of the ductile layer (Table 2). Using a characteristic scale factor for density (~0.5), for length (1.5×10^{-7}) and for viscosity (~$5–7 \times 10^{-18}$), we estimate that 1 hour of experiment corresponds to about 1 Myr in nature, and that the velocity of the piston in the experiment (~0.44 cm h^{-1}) corresponds to ~2.5 cm yr^{-1} (Table 2). The viscosity ratio between the lithosphere ($\eta_{|o}$) and the upper mantle ($\eta_{|m}$) is equal to about 300–400 in our experiments. It is difficult to relate these values to natural ratios, because the effective viscosity value used in our experiments represents an attempt to model the complex and nonlinear rheology laws that govern the lithosphere with simple viscous flow. Similar viscosity contrasts, however, have been commonly used in previous simulations [e.g., *Kincaid and Olson*, 1987; *Houseman and Gubbins*, 1997; *Becker et al.*, 1999; *Conrad and Hager*, 1999]. The density contrast between the lithospheric plates and the underlying mantle is chosen to respect the range of natural values as discussed in section 2.2.

2.2. Forces at Work

[16] Evaluation of the different forces that act in subduction/collisional systems is difficult to operate both in nature and in experiments [*McKenzie*, 1969; *Forsyth and Uyeda*, 1975]. The collisional process initiates when the horizontal compressional stress overcomes the strength of the lithosphere [*Davy and Cobbold*, 1991]. However, if the contact between the two continental plates is preceded by the consumption of oceanic lithosphere, the horizontal compressional stress should also overcome the vertical load exerted by the subducting material. This load, in turn, is function of the slab's rheological properties. In the following we review the main forces that act in natural and laboratory systems.

2.2.1. Driving Forces

[17] In our experiments, two main driving forces explain the development of the subduction zone: the slab-pull force (F_{sp}) arising from the weight of the descending slab, and the horizontal compression arising from the advance of the piston (D_r).

2.2.1.1. Slab-Pull Force (F_{sp})

[18] A mature oceanic lithosphere is gravitationally unstable with respect to the underlying mantle. After the for-

Table 1. Physical Parameters and Some Results of Experiments

	Experiment							
	1[a]	2	3	4	5	6[a]	7[a]	8
Thickness, 10^{-3} m								
Silicon layers H_{sil}	9	9	9	9	9	9	14[a]	9
Sand layers H_{sand}	3	3	3	3	1–1.5[a]	3	5[a]	1.5–2[a]
Honey H_m	99	100	166[a]	183	180	168	168	180
Length, 10^{-3} m								
Southern continent L_{cs}	200	200	240	200	205	200	230	230
Ocean L_o	70	70	70	30[a]	100	70	50	70
Northern continent L_{cn}	230	230	190	190	200	230	220	200
Viscosity, Pa s								
Oceanic silicone η_o	1.8×10^5	1.6×10^5	1.5×10^5	1.5×10^5	1.6×10^5	1.8×10^5	1.8×10^5	1.6×10^5
Continental silicone η_c	1.4×10^5	1.4×10^5	1.0×10^5	1.0×10^5	1.0×10^5	1.4×10^5	1.4×10^5	2.3×10^5
Honey η_m	4.6×10^2	4.6×10^2	4.6×10^2	4.6×10^2	4.6×10^2	4.6×10^2	4.6×10^2	4.6×10^2
Density, kg m^{-3}								
Oceanic silicone ρ_{osil}	1480	1454[a]	1465	1465	1476	1470	1480	1476
Oceanic sand ρ_{osand}	1500	1500	1500	1500	1500	1500	1500	1500
Continental silicone ρ_{csil}	1324	1324	1296	1348	1348	1304	1310	1348
Continental sand ρ_{csand}	1300	1300	1300	1300	1500	1250	1250	1300
Honey ρ_m	1425	1425	1425	1425	1425	1425	1425	1425
Time								
Piston velocity u, m s^{-1}	1.2×10^{-6}	1.2×10^{-6}	1.2×10^{-6}	1.2×10^{-6}	1.2×10^{-6}	1.2×10^{-6}	1.2×10^{-6}	1.2×10^{-6}
Total duration, hours	68.5	50.5	50.9	69	53	71.5	67	70
Dimensionless Numbers								
F_1	0.98	0.68	0.86	0.37	1.94	0.85	0.53	1.24
F_2	2.34	1.76	4.01	4.35	4.33	3.45	6.19	4.42
Results								
Amount of continental subduction, mm	60	>68	28	43	15	40	12	18
Equivalent in nature, km	400	450	190	290	100	270	50	120
Ocean closure time, hours	30	30	25	16	31	33	12	24
Bottom-slab interaction, hours	26	35	23	32	11/28	18	17	21
Collision time, hours	52	>55	34	30	37	46	16	30

[a]Parameters that differ significantly from the previous experiments.

mation of an initial instability, the density contrast between the oceanic lithosphere and the mantle becomes the main engine of subduction [*McKenzie*, 1977]. The pulling force F_{sp} that results from the negative buoyancy of the oceanic slab is proportional to the density contrast $\Delta\rho_{o\text{-}m}$ between lithosphere (ρ_o) and mantle (ρ_m), to gravity (g), and to the depth (z) and thickness (H) of the slab. The density contrast is not constant but depends on the age of the oceanic lithosphere and on the phase changes that occur within the slab during subduction [e.g., *Vlaar and Wortel*, 1976; *Turcotte and Schubert*, 1982; *Bina*, 1996, 1997; *Marton et al.*, 1999; *Schmeling et al.*, 1999].

[19] In the experiments, thermal buoyancy of the oceanic lithosphere is simulated by imposing a density contrast $\Delta\rho_{o\text{-}m}$ between the oceanic lithosphere and the underlying mantle ranging from 40 to 60 kg m^{-3} (Table 1). We neglect the role of endothermic phase changes at the transition zone.

[20] The maximum slab-pull force depends on the initial length of oceanic plate, that is varied in our experiments from an equivalent of 200 to 700 km, and on the depth of the high-viscosity lower mantle, that is varied from 660 km to 1100 km, covering a large number of examples of tomographic images of subducting slabs [e.g., *Karason and van der Hilst*, 2000]. F_{sp} increases with the length of the slab and reaches an equivalent of roughly 4×10^{13} N m^{-1} for a 660-km-long slab, consistent with other estimates [*McKenzie*, 1977; *Davis*, 1980; *Turcotte and Schubert*, 1982].

[21] The entrance at trench of continental material results in a variation of the force equilibrium. In particular, we expect a decrease in the negative buoyancy of the system due to the subduction of buoyant continental lithosphere. In natural systems, the continental lithosphere can be either negatively or positively buoyant depending on crustal thickness [*Cloos*, 1993; *Ranalli*, 2000]. A reference continental lithosphere, however, is less dense than the mantle by about 50 to 100 kg m^{-3}. In the experiments, the continental lithosphere is less dense than the mantle by about 100 kg m^{-3}.

[22] As discussed above, we do not explore mineralogical phase changes during subduction, which may result in a strong increase of the continental density and facilitate continental subduction. The scrape off of crustal buoyant material from the dense mantle lithosphere may also favor the ability of the delaminated continent to subduct [*Chemenda et al.*, 2000], although this possibility is limited to the case of hot lithospheric plates [*Ranalli*, 2000]. Our experimental setup does not include low-viscosity lower crust and, consequently, does not permit delamination. For these reasons, our results should be considered as lower bound values when estimating the possible amount of continental subduction.

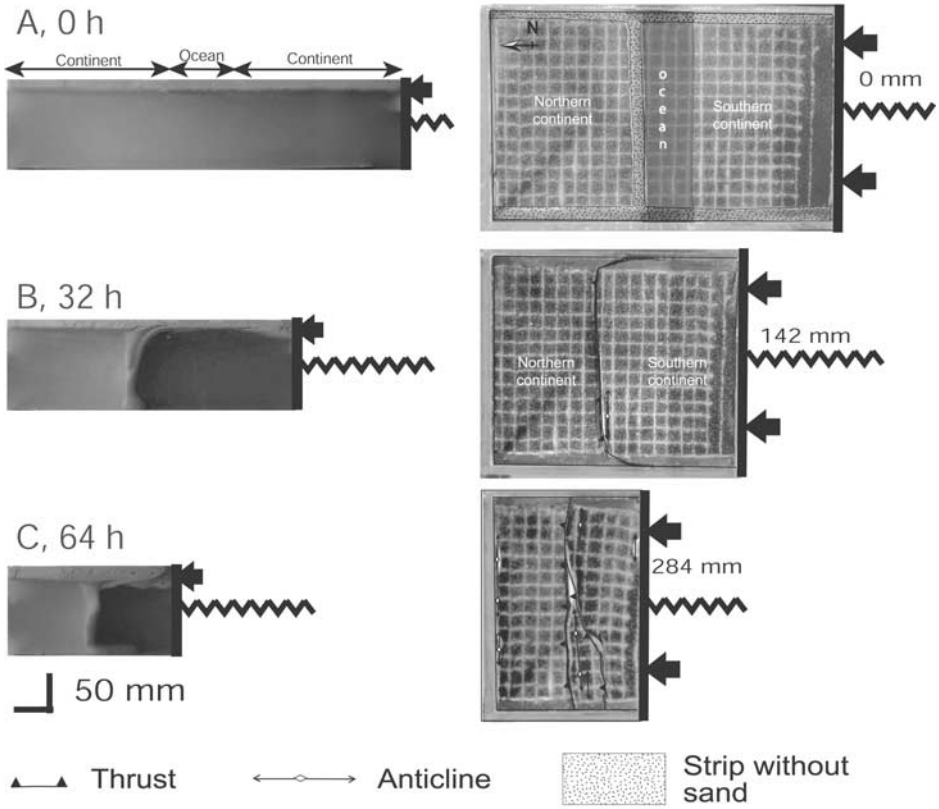

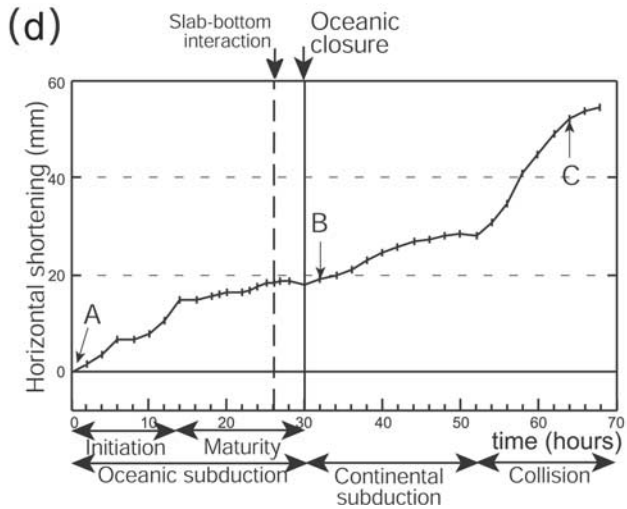

Figure 2. (a–c) (left) Lateral views and (right) top views of experiment 1. The displacement of the piston is indicated at the right of top views. The strip without sand favors the beginning of subduction at the northern ocean-continent boundary. After 16 hours of experiment, the slab is forming. After 32 hours, it has yet reached the bottom of the box. Collision begins between 48 and 64 hours and is marked by the formation of folds and thrusts. (d) Shortening versus time in experiment 1. We report here the total shortening occurring within the plates, excluding the shortening accommodated at the subduction zone. This intraplate shortening is estimated calculating the variation of the distance between the boundaries of the model and the closest grid lines parallel to the trench. We also indicate the timing of Figures 2a–2c. Oceanic closure marks the beginning of continental subduction. Continental subduction is characterized by low shortening rates, all the advance of the piston being absorbed at trench by the subduction zone. Collision, characterized by the widespread development of folds and thrusts within the continents, starts after 22 hours of continental subduction.

Table 2. Scaling of the Physical Parameters of Experiment 1

Quantity	Symbol	Nature	Model	Scaling Ratio Model/Nature
Length, m	L			
Lithosphere thickness	H	8.0×10^4	0.012	1.5×10^{-7}
Depth of transition zone	Z	6.6×10^5	0.11	1.7×10^{-7}
Gravity, m s^{-2}	g	9.81	9.81	1
Density, kg m^{-3}	ρ			
Oceanic lithosphere	ρ_o	3370	1485	0.441
Continental lithosphere	ρ_c	3200	1318	0.412
Mantle	ρ_m	3300	1425	0.432
Density contrast (ρ_o-ρ_m)	$\Delta\rho_{o\text{-}m}$	70	60	0.857
Density contrast (ρ_c-ρ_m)	$\Delta\rho_{c\text{-}m}$	−100	−107	1.070
Density ratio	ρ_o/ρ_m	1.021	1.042	
Density ratio	ρ_c/ρ_m	0.970	0.925	
Viscosity, Pa s	η			
Ocean	η_o	2.50×10^{22}	1.8×10^5	7.2×10^{-18}
Continent	η_c	2.50×10^{22}	1.4×10^5	5.4×10^{-18}
Mantle	η_m	10^{20}	4.6×10^2	4.6×10^{-18}
Viscosity ratio	η_o/η_m	2.5×10^2	3.9×10^2	
Viscosity ratio	η_c/η_m	2.5×10^2	3.0×10^2	
Friction coefficient of brittle layer	μ	0.6	0.6	1
Characteristic time, equal to $\eta_o/\sigma_o = \eta_o/\rho_o gl$, s	t	$3.4 \times 10^{13} \approx 1$ Myr	3600 = 1 hour	1.05×10^{-10}
Convergence velocity, m s^{-1}	u	$7.8 \times 10^{-10} \approx 2.5$ cm yr^{-1}	$1.2 \times 10^{-6} = 4.4$ mm h^{-1}	1.5×10^3

2.2.1.2. Other Driving Forces

[23] The second type of forces (D_r) arise from the cooling oceanic lithosphere (ridge push), and from the basal drag acting under the oceanic plate. Published estimates of the ridge push range between 3 and 7×10^{12} N m^{-1} depending on the cooling models [*Parsons and Richter*, 1980]. Less precise estimations are available for the basal drag [cf. *Forsyth and Uyeda*, 1975; *Hager and O'Connell*, 1981]. *Muller and Phillips* [1991] consider that basal drag can induce in-plane compressional stress in the order of 10^{12} N m^{-1} per 1000 km of application. The combined effect of the basal drag and ridge push should be smaller than the slab-pull force, except in particular situations, such as during the initiation of subduction.

[24] In the experiments, we simulate compressive forces by using a piston advancing at constant rate. Deformation is driven for about 2–3 days, equivalent to geological times of 40–70 Myr, with an equivalent shortening of 1000–2000 km. The rate of shortening corresponds to about 2.5 cm yr^{-1}.

2.2.2. Forces Resisting Subduction

[25] These forces result mainly from the resistance opposed by the oceanic lithosphere to deform at oceanic trenches, and from the resistance opposed to slab penetration into the mantle.

2.2.2.1. R_b, Bending Resistance

[26] The force necessary to bend the plate at the trench has been identified in mature stages of subduction as one of the main resisting forces controlling the subduction process [*McKenzie*, 1977; *Houseman and Gubbins*, 1997; *Becker et al.*, 1999; *Conrad and Hager*, 1999]. It is directly proportional to the viscosity of the lithosphere (η_o), to its velocity (u) and to the cube of its thickness (H), and inversely proportional to the cube of the radius of curvature of the subducting plate (r) [*Turcotte and Schubert*, 1982; *Becker et al.*, 1999].

2.2.2.2. R_f, Fault Resistance

[27] Resistance to sliding along the subduction fault (R_f) is considered as another important parameter. Computations of the shear friction range between 15 and 30 MPa [*Zhong and Gurnis*, 1994; *Tichelaar and Ruff*, 1993]. It may contribute for about 30% of the energy dissipated during subduction [*Conrad and Hager*, 1999]. *Faccenna et al.* [1999] estimate this force for a model setup similar to the one we use here.

2.2.2.3. R_s, Mantle Resistance

[28] Finally, the shear force (R_s) at the slab-mantle interface is proportional to the mantle viscosity (η_m) and to the subduction velocity (u). It increases strongly in the lower mantle, where the viscosity is at least 1 order of magnitude larger than in the upper mantle [*Hager*, 1984; *Gurnis and Hager*, 1988; *Lambeck et al.*, 1990; *Davies and Richards*, 1992; *Lithgow-Bertelloni and Richards*, 1998]. Since the upper mantle viscosity is 2 orders of magnitude lower than that of the lithosphere in the experiments (Table 1), the resisting force is negligible with respect to that of the bending force [*Becker et al.*, 1999; *Conrad and Hager*, 1999].

2.2.3. Forces at Work During Subduction and the Deformation of the Slab

[29] This force equilibrium can be greatly modified by the deformation of the slab. Gravitational forces generate deviatoric stresses acting on the subducting slab and promote down-dip extension in the upper part of oceanic slabs, as imaged by focal mechanisms [*Isacks and Molnar*, 1971; *Spence*, 1987; *Zhou*, 1990]. If a slab detaches from lithosphere and sinks into the mantle, the slab-pull force diminishes and this will affect the dynamics of subduction.

[30] There are two possible modes of slab detachment.

[31] 1. Extension forces in the slab eventually result in slab break-off, when they are large enough to overcome the strength of the entire subducting slab [*van den Beukel*, 1992; *Davies and von Blanckenburg*, 1995; *Yoshioka and Wortel*, 1995; *Wong A Ton and Wortel*, 1997]. Published numerical simulations show that slab detachment is expected to occur following subduction and during the early stages of continental collision.

[32] In our experiments, the strength of the slab is mainly controlled by the thickness of the sand layer, and it can be estimated from the strength envelope of sand. Supposing that an eigenvector of the stress tensor within the slab is perpendicular to the subduction plane and that the corre-

sponding eigenvalue is the hydrostatic pressure, then the force necessary to break the sand layer and to achieve slab break-off in our experiments is the integrated stress necessary to overcome Mohr-Coulomb yield stress. This force is proportional to the thickness of the sand layer (H_{sand}), to the hydrostatic pressure for the depth at which slab detachment occurs (P), and to a parameter (α) related to the friction coefficient μ of the sand ($\mu = \tan 30°$; $\alpha = 2\mu/\mu + (1 + \mu^2)^{1/2}$)) The mathematical expression for α is obtained using the Mohr-Coulomb criterion for a cohesionless material. The strength associated to stretching of the silicone layer is $\eta_\sigma\, d\varepsilon/dt\, H_{sil}$, where $\varepsilon\eta_o$ is the viscosity of the oceanic plate silicone, $d\varepsilon/dt$ is the applied strain rate and H_{sil} is the thickness of the silicone layer. Considering that the length of the stretched zone during the slab break-off is roughly equal to the thickness of the slab, we obtain the force necessary to achieve the rupture of the slab ($F_{rupture}$):

$$F_{rupture} = \alpha\rho_m\, gHH_{sand} + \eta_o\, u\, H_{sil}/H, \quad (1)$$

where u is the convergence velocity, ρ_m is the mantle density, g is the gravity, and H is the total thickness of the lithosphere ($H = H_{sand} + H_{sil}$).

[33] The slab-pull force in experiments is controlled by the length of the subducting oceanic plate. The vertical tension in the slab results from the negative buoyancy of the oceanic part of the slab, and from the positive buoyancy of the subducted continent. Its amplitude is limited by the depth of the convective mantle layer or by the length of the oceanic plate if it is smaller than the mantle depth. The maximum tension force F_T within the slab can be normalized with $F_{rupture}$ to define a dimensionless number F_1. If the initial length of the oceanic plate L_o is larger than the depth of the mantle Z, this number is

$$F_1 = F_T/F_{rupture} = (\Delta\rho_{o\text{-}m}\, g\, Z\, H)/F_{rupture}, \quad (2)$$

where $\Delta\rho_{o\text{-}m}$ is the density contrast between the oceanic lithosphere and the mantle.

[34] If L_o is much smaller than Z, F_1 is

$$F_1 = (\Delta\rho_{o\text{-}m}\, g\, L_o\, H)/F_{rupture}. \quad (3)$$

F_1 characterizes the possibility for the slab to break under its own weight.

[35] 2. Gravity forces can also produce deformation in the viscous part of the slab, and generate a Rayleigh-Taylor type gravitational instability [*Houseman et al.*, 1981; *Buck and Toksöz*, 1983; *England and Houseman*, 1989; *Lenardic and Kaula*, 1995; *Conrad and Molnar*, 1997; *Houseman and Molnar*, 1997; *Molnar et al.*, 1998; *Neil and Houseman*, 1999; *Pysklywec et al.*, 2000]. The time necessary to achieve the formation of this instability is controlled by the negative buoyancy and viscosity of the mantle lithosphere, and the wavelength of the instability. In our experiments, we observe the formation of viscous instabilities during subduction. We find that the time necessary to achieve the instability is proportional to $\eta_o/\Delta\rho_{o\text{-}m}gH_{sil}$, where η_o is the viscosity of the oceanic plate. We define a second dimensionless number,

$$F_2 = Z\,\Delta\rho_{o\text{-}m}\, g\, H_{sil}/u\,\eta_o. \quad (4)$$

F_2 characterizes the possibility for a viscous instability affecting the oceanic slab to develop before the slab reaches the bottom of the convective layer. If F_2 is large, viscous instabilities should be able to develop during subduction.

[36] The possibility for the oceanic slab to deform during subduction has important consequences on continental subduction, because it may drastically change the slab-pull force. In the following, we present analogue experiments in which both F_1 and F_2 vary.

3. Experimental Results

[37] Experiments have been set up to test the influence of two parameters that we consider important in understanding the initiation of the collisional process. In detail, we test the role (1) of the slab-pull force resulting from the subduction of the oceanic lithosphere and (2) of the strength of the slab. The first parameter has been investigated by varying the density contrast (experiment 2), the length of the oceanic plate (experiment 4), or the thickness of the oceanic lithosphere (experiment 7) (Table 2). The strength of the slab is tested by changing the layering of the oceanic lithosphere, which influences F_1. Increasing the slab-pull force results in an increase of F_1, while F_2 varies primarily as a function of the depth of the mantle. Eight experiments have been performed. The complete description of their physical parameters is available in Table 1. In the following, we describe four experiments that we selected because they illustrate the different kind of possible slab evolution, depending of the physical properties of the slab. The other four experiments confirm the interpretations deduced from those descriptions, and they are considered in the final discussion.

3.1. Experiment 1

[38] Experiment 1 has been set up with a convective mantle depth equivalent to 660 km and with a relatively thick (3 mm) sand layer on the oceanic lithosphere. This results in relatively low F_2 and F_1 parameters (Table 1). This setting decreases the possibilities for the slab to deform or break during subduction.

[39] The experimental evolution shows four different stages:

[40] 1. The first stage is initiation of oceanic subduction (Figure 2). During the first 14 hours of experiment, the weak passive margin is inverted with the development of compressional structures that appear also at the box boundaries (Figure 2). Then a slab-like instability grows at depth below the margin, as already described by *Faccenna et al.* [1999]. About 30% of the total shortening is accommodated outside the plate margin, in the intraplate domain (Figure 2). This compressional deformation is mostly localized at the piston-plate border and is possibly related to an initial heterogeneity. This shortening also indicates that, at this moment, the slab-pull force exerted by the instability is still not large enough to overcome the resistance at trench [*Faccenna et al.*, 1999].

[41] 2. The second stage is the development of the slab (Figure 2; 14–30 hours of experimental run). The length of the slab increases progressively (Figure 2, left). The tip of the slab reaches the bottom of the mantle after 11 cm (~26 hours) of shortening. During this phase, shortening is mainly accommodated at the trench (Figure 2d) and the

average velocity of subduction is similar to the velocity of the piston, indicating that at that time, subduction is mainly driven by the push of the advancing piston and subordinately by the negative buoyancy of the subducted material.

[42] 3. The third stage is the initiation of continental subduction (Figure 2). The oceanic closure is achieved after 30 hours of experiment and is followed by subduction of the continental plate for about 20 hours. We note that the entrance of buoyant continental material at the trench does not produce any shortening on the surface. All the shortening is transmitted into the well developed trench. The average buoyancy of the slab is still negative at this time, because part of the hanging slab is still composed of the previously subducted dense oceanic material. The trench moves toward the north, while the slab preserves its subvertical geometry. The continuation of subduction results in the flattening of the slab at the bottom of the box. As the trench-slab couple moves to the north, the deep flat slab portion rests to the back of the slab. During this period, 90% of the shortening produced by the advancing piston is accommodated at the trench (Figure 2d). Taking into account surface shortening and erosion at the trench of the overriding continental plate, we evaluate that 6 cm of positively buoyant continental material enters at trench. This corresponds to an equivalent of about 400 km of continental subduction (Table 1).

[43] 4. The fourth stage is collision. After 52 hours, the deformation regime changes and compressional structures (folds and thrusts) appear. They develop particularly within the southern continent. Forty-five percent of the shortening produced by the advancing piston is accommodated by these surface compressional structures, some continental material being still pushed into the subduction zone. The sharp decrease in the continental subduction rate and the corresponding increase in surface shortening mark the initiation of collision.

[44] Experiment 2 is set with similar boundary conditions to that of experiment 1, but with a lighter oceanic plate (Table 1). Its evolution is similar, continental subduction being active during more than 22 hours. This suggests that the driving force controlling subduction is mainly produced by the advance of the piston. This experiment has been stopped before the onset of collision.

3.2. Experiment 3

[45] Experiment 3 has been set up to test the role of the depth of the mantle. Indeed, the major difference between this experiment and experiment 2 is the thickness of the mantle layer that has been increased to 18 cm, corresponding to 1100 km in nature (Table 1). Therefore the dimensionless number F_2 is larger, which should favor the genesis of viscous instabilities. In contrast, F_1 does not change significantly (Table 1).

[46] As observed in the previous experiment, the initiation of subduction (between 0 and 14 hours of experiment) is accompanied by the development of compressive structures (Figure 3). The compressional deformation is mostly localized at the weak plate margin and only 10% of the total shortening is distributed outside this area. After 14 hours, the newly formed oceanic slab subducts rather steeply into the mantle at the velocity of the piston (Figure 3). Between 20 and 24 hours, the slab thins in its middle portion. After about 24 hours, part of the slab flows down to the bottom of the box (Figure 3). We observe that the drip involves only silicone. This viscous drip remains attached to the slab by a thin silicone thread, a morphology typical of the Newtonian behavior of the silicone. The formation of the silicone drip does not result in any immediate change of the surface strain regime. Oceanic subduction pursues while shortening localizes at trench. The volume of the silicone drip (measured at the end of the experiment) is about 182 cm^3, corresponding to more than 90% of the initial volume of the oceanic silicone slab.

[47] After 25 hours of experiment, continental material enters the trench and subducts during about 9 hours before horizontal shortening and collision initiates. At that time, taking into account the continental erosion, 28 mm of continental plate has been subducted, which would correspond in nature to 190 km. This value is significantly smaller than that of the previous experiments. The formation of the viscous drip is probably responsible for the smaller amount of subducted continental plate before the onset of collision. As a matter of fact, the removal of dense silicone from the slab significantly decreased the slab-pull force capable to pull down the buoyant continental material.

3.3. Experiment 4

[48] Experiment 4 has been performed to test the influence of the length of the oceanic plate. In this experiment we decrease the length of the oceanic plate by 60% with respect to experiment 3 (Table 1). As a consequence, F_1 is smaller while F_2 has a similar value than in experiment 3. The initial evolution of the experiment is similar to that observed in experiment 3. The closure of the oceanic basin occurs after 16 hours. It is followed by about 14 hours of continental subduction without any compressional surface deformation (Figure 4). After 30–32 hours of experiment, a viscous instability develops, falls rapidly down to the bottom of the box and removes about 85% of the volume of dense silicone. Soon after, the rate of surface shortening increases sharply and collision starts. This experiment clearly shows the role of the slab-pull force on the initiation of collision. The amount of continental lithosphere that is able to subduct before the initiation of collision depends on the amount of oceanic lithosphere that has been previously subducted. In experiment 4, however, the silicone drip forms after the entrance in the trench of the continent, whereas in the previous experiment 3, it has formed before the onset of continental subduction. Hence we observe that the former subduction of a larger oceanic domain does not necessarily result in the subduction of a larger amount of continental material, because part of the oceanic slab may detach and cause a decrease in the slab-pull force.

3.4. Experiment 5

[49] To test the influence of the strength of the slab, experiment 5 is set by decreasing the oceanic sand layer thickness by about 50% (1.5 mm) with respect to experiment 3. We also increase the length of the oceanic plate by about 40%. F_1 increases significantly with respect to experiment 3, while F_2 remains constant. The reduction of the sand layer's thickness produces a significant weakening of the oceanic plate, which may now deform internally during the initial phases of shortening. To avoid the internal

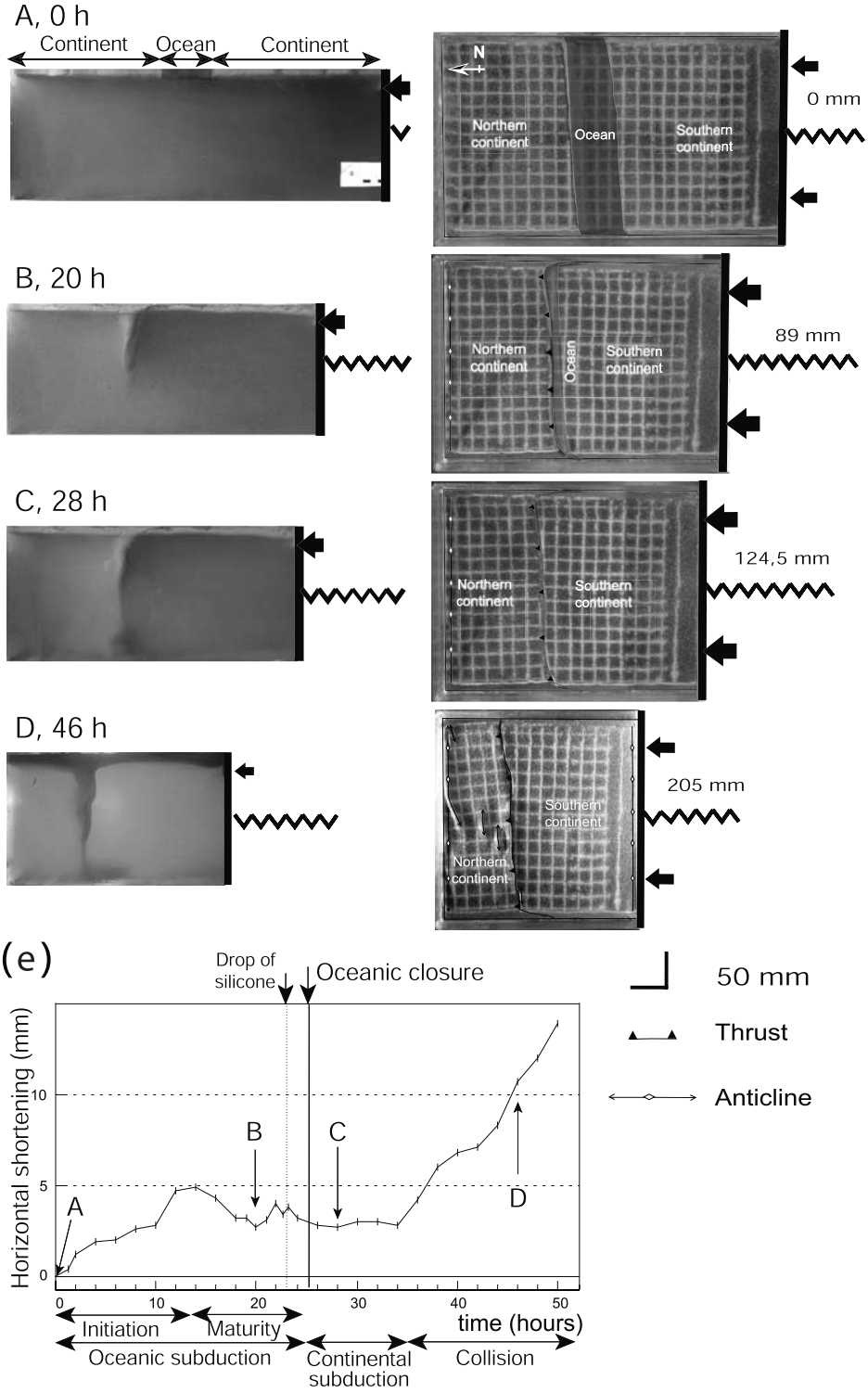

Figure 3. (a–d) (left) Lateral views and (right) top views of experiment 3. See Figure 2 caption for explanations. Oceanic closure is achieved at around 25 of experiment. (e) Shortening versus time in experiment 3. See Figure 2d caption for explanations. The drop of dense silicone occurs at around 23 hours of experiment. In this experiment, continental subduction lasts only 9 hours, significantly less than in the previous ones, because the drop of silicone diminished the slab-pull force exerted by the oceanic slab.

deformation of the plate and to ensure a rapid development of the slab, we initially place a dense silicone strip (0.9 thick and 1.5 cm large) beneath the weak margin, in order to simulate an existing subduction zone. The initial configuration of this experiment reproduces the early stages (4 hours) of subduction of the previous experiments.

[50] After 11 hours, 75% of the shortening localizes at the trench, while the rest is localized immediately in front of the

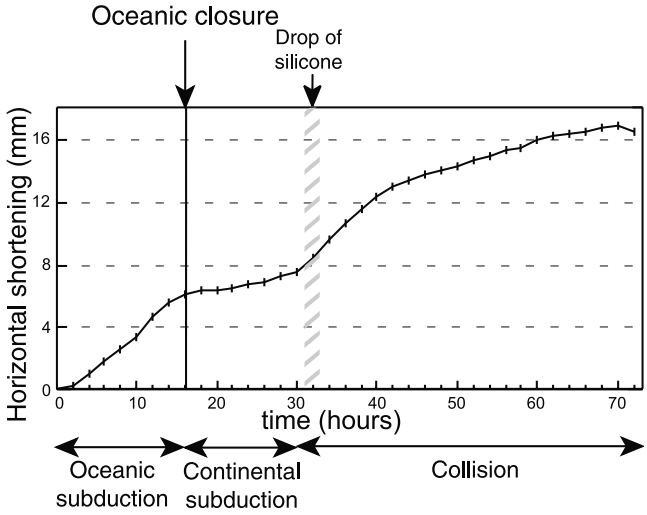

Figure 4. Shortening versus time in experiment 4. Continental subduction lasts 14 hours, and collision initiates when the silicone drip detaches from the slab, which results in an increase of the average slab buoyancy.

piston (Figure 5). A first silicone drip forms at that time. The partitioning of deformation between the trench and the intraplate domains pursues for another 11 hours. After 22 hours of experiment, surface shortening stops and is followed by extension. The extension rate progressively increases with time as a result of the increased amount of subducted material. Taking into account of erosion of the overriding plate, we estimate that during this time interval the trench retreats by about 2 cm. Therefore, between 22 and 35 hours, the velocity of subduction is higher than that of the piston. This effect results from the large slab-pull force with respect to the strength of the lithospheric plate, in comparison to previous experiments.

[51] The continent arrives into the trench after 31 hours. Surface horizontal extension, however, remains active (Figure 5), although at a lower rate. After about 38 hours of experiment, the slab stretches and finally breaks (Figure 5). The rupture is approximately localized at the continent-ocean margin, separating the heavy (oceanic) lower part from the upper lighter part of the slab. After the break-off, the lower dense slab rapidly sinks down to the bottom of the box, while the attached light upper part of the slab folds and moves back. After the break-off, the surface tectonic regime changes drastically and collision starts. In the later stages of the experiment the continental slab moves upward to finally lie under the overriding continental plate.

[52] This experiment differs from the previous one in that the weak oceanic slab breaks off. This process causes a sudden decrease in the slab-pull force. Only an equivalent length of 100 km of continent has subducted. This amount of continental subduction is much smaller than in the previous experiments, especially in the experiments for which the slab does not drip or detach at depth.

4. Interpretation of Experimental Results

[53] All these experiments share common features of evolution, from the first episodes of deformation to the final stages of continental collision. On the surface, a first episode of shortening always occurs during the initiation of subduction. In fact, the weaker of the two continental margins becomes active and accommodates most of the shortening imposed by the piston. Nevertheless, some shortening also occurs in the other continental margin and near the piston. This happens until the viscous instability below the northern continental margin adopts the shape of a slab, which occurs after an equivalent amount of 150–200 km of subduction. From this moment, the load of the subducted slab is large enough to overcome the resisting forces acting at the newly formed trench, where shortening is transmitted [*Faccenna et al.*, 1999; *Becker et al.*, 1999]. The formation and development of the slab is characterized by a progressive and exponential increase in the rate of subduction, associated with an increase in length of the slab. The average velocity of subduction is similar to the velocity of the piston. Only in experiment 5, the subduction velocity is higher than convergence velocity. In this experiment, indeed, the ratio of the slab-pull force and the strength of the lithospheric plate (F_1) are larger. As a result, the trench of the slab retreats backward and produces back arc extension.

[54] The closure of the oceanic basin and the entrance into the trench of buoyant continental material never produces an immediate tectonic response on the surface. The steep morphology of the trench is preserved. Surface shortening only occurs after a certain amount of continental subduction. The onset of this shortening episode is defined here as the onset of collision. As the trench locks, its depressed topography disappears, and the advance of the piston is accommodated by a thrust and fold belt that initially localizes near the convergent margin.

[55] The amount of subducted continent before the onset of collision is variable and depends mainly on the maximum slab-pull force attained by the subducted slab. As the piston continues to push the trailing edge of the continental plate into the trench, continental subduction may also pursue when the system is neutrally buoyant. Hence collision effectively starts when the subducting system attains a significant positive buoyancy. It is difficult to give an exact estimate of this value, but we expect that collision initiates when a threshold value of positive buoyancy has been attained. This value should depend on the equilibrium between the buoyancy level in the mantle, the resisting force at the trench and the boundary push. The amount of light continental material needed for the system to attain this threshold positive value depends on the length of the subducted portion of oceanic lithosphere actively pulling down the buoyant continental plate.

[56] We test different configurations by varying the original length of the ocean and the thickness of the mantle and the rheology of the slab. We note that the rheological characteristics of the slab are important, in that they control the possibilities for the slab to deform under its own weight. Particularly, long or weak hanging slabs are likely to deform by viscous removal of their denser parts, with the formation of a Rayleigh-Taylor type instability or by slab break-off. Slab deformation produces a decrease in the slab-pull force, reducing the amount of continental lithosphere that can be subducted before the plates collide. If the slab is strong or/and the amount of hanging dense material is small, the slab does not deform and remains attached to the continental subducting plate. In this case, the slab-pull force remains

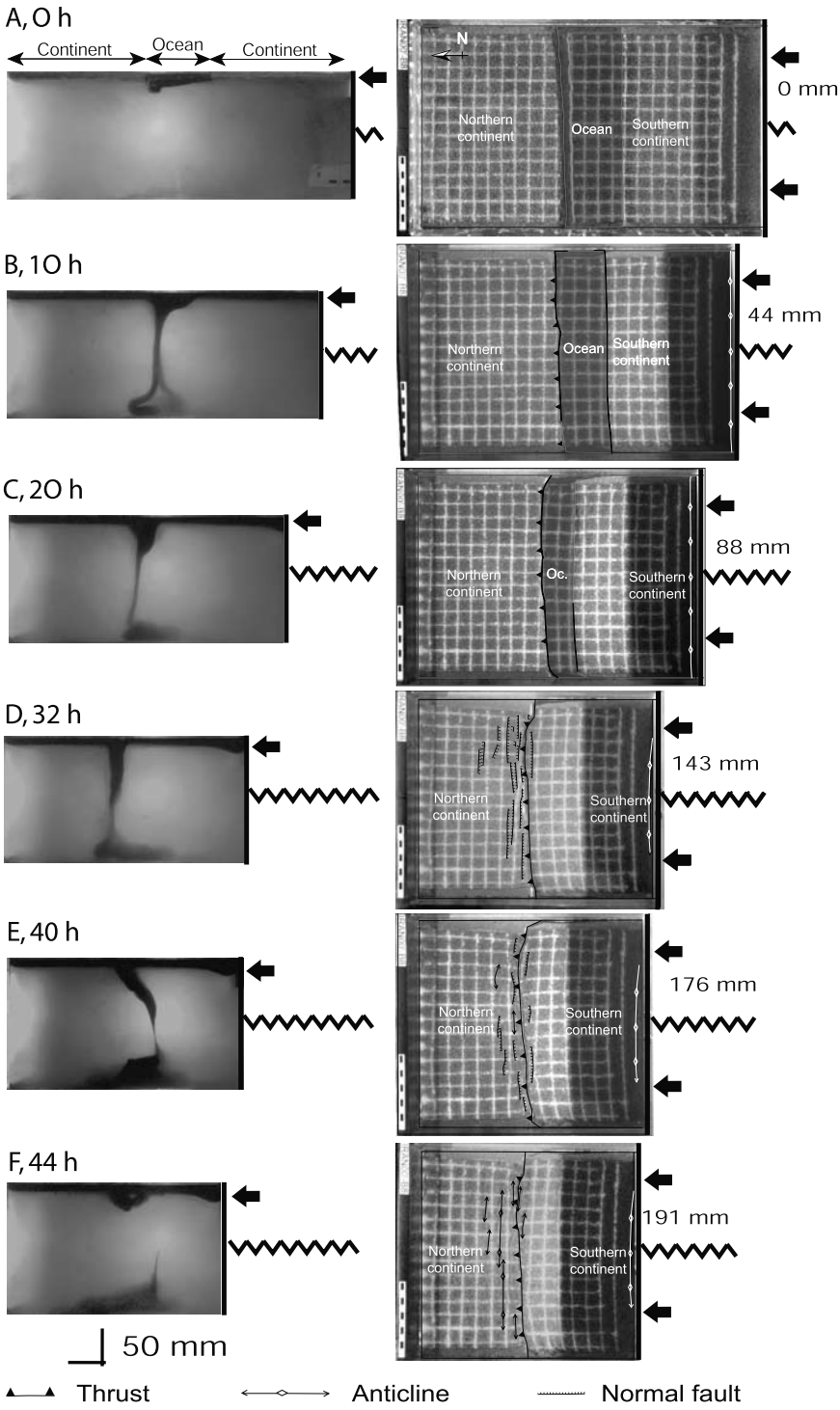

Figure 5. (a–f) (left) Lateral views, (right) top views, and (g) shortening versus time for experiment 5. See Figure 2 caption for explanations. After 20 hours of experiment, the slab resembles that of experiment 3 after 20 hours (compare Figure 3). The mature stage of oceanic subduction is marked by horizontal extension, horsts and grabens appearing in the northern continent. The oceanic domain closes after 32 hours of experiment and continental subduction is active during 5 hours. Note that the horizontal extension pursues after the beginning of continental subduction. The break-off of the slab, which occurs after 37 hours of experiment, results in the onset of collision, which is marked by the growth of folds and thrust faults reactivating the old extensional structures. Folds can be seen yet at 40 hours even if the former extensional structures are mainly visible at that time.

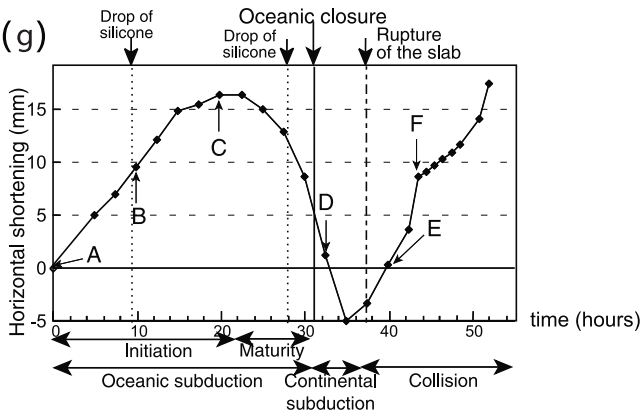

Figure 5. (continued)

active until a large portion of continental lithosphere has been subducted to compensate the negative buoyancy of the oceanic part of the slab.

[57] Comparison between models 1 and 3 shows that the formation of a viscous instability is favored if mantle circulation is open at a depth larger than 660 km. This derives from the imposed rheology of the slab. Newtonian deformation, in fact, produces deformation that is more diffuse than non-Newtonian rheologies. Hence the thinned portion of the slab is quite large and the tip of the slab may arrive to the box bottom boundary before the slab has stretched enough to lose its continuity.

[58] Figure 6 summarizes the experimental results in terms of the two dimensionless parameters F_1 and F_2. These parameters characterize the possibility for the slab to break under its own weight (large F_1), and the appearance of a viscous instability (large F_2). We observe that viscous drips appear in our experiments for F_2 larger than about 3, whereas slab rupture has been observed in experiments where F_2 is larger than 3 and F_1 is larger than about 1. Low F_1 and F_2 values, in contrast, correspond to models in which the slab does not deform significantly. We do not present any experiment characterized by a low F_2 and a high F_1 parameter. Such experiments, however, have been realized by *Funiciello et al.* [2001], although with somewhat different boundary conditions (see below). In such experiments, the slab does not deform much, although the high F_1 parameter shows that the slab-pull force could theoretically achieve slab rupture. As a matter of fact, the F_2 parameter being too small, the viscosity of the slab delays the deformation of the slab, and the lithospheric plate reaches the bottom of the box before the slab has been significantly stretched.

[59] We observe that the episode of continental subduction, that begins with the closure of the oceanic domain and that ends with the onset of collision, may last between 4 and 22 hours, equivalent to an interval of time ranging from 4 to 22 Myr (Table 2 and Figure 6). The corresponding equivalent length of continental subduction ranges from 50 to 450 km. The larger F_1 and F_2, the smaller the amount of continental subduction. When F_2 is large, instabilities that result from the removal of dense viscous parts of the slab

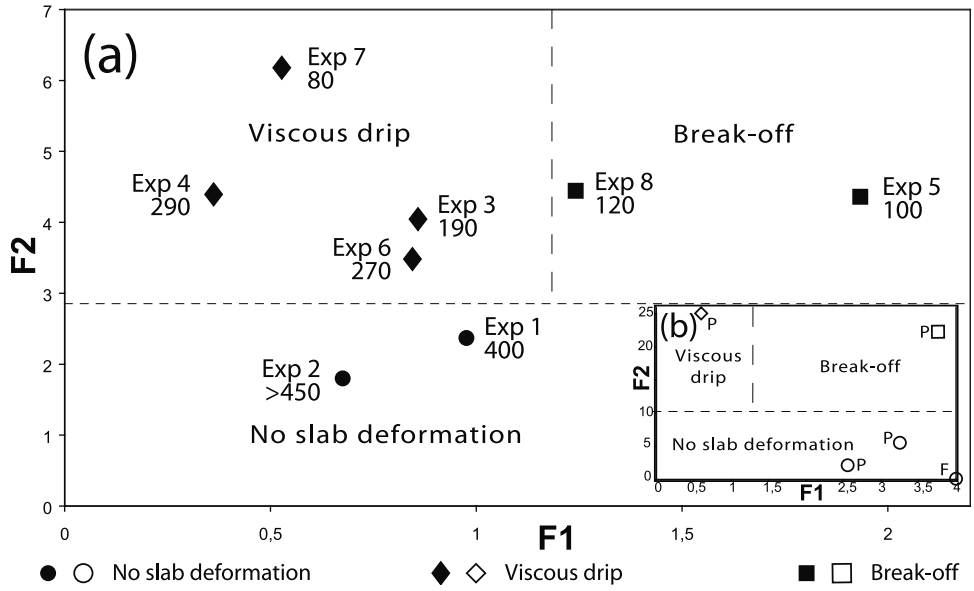

Figure 6. (a) F_1 and F_2 dimensionless parameters for the set of experiments described in this paper. Circles mark experiments in which neither viscous drip nor break-off occurred (small F_1 and F_2 parameters), diamonds mark experiments with viscous drip but without any break-off (large F_2 and small F_1), and squares mark experiments with break-off (large F_1 parameter). Three domains have been highlighted. Low F_2 characterizes experiments without deformation. High F_2 characterizes experiments showing slab deformation: high F_1/high F_2, break off occurs; low F_1/high F_2, drip development only. The equivalent length in km of subducted continental lithosphere before the onset of collision is indicated near the corresponding symbols. Both viscous drips and slab break-off decrease the slab-pull force and diminish the amount of continental subduction. (b) Same as Figure 6a for the experiments described by F, *Funiciello et al.* [2001], and P, *Pysklywec et al.* [2000].

decrease the slab-pull force, reducing the amount of subducted continental material before the onset of collision. When F_1 is large, the entire slab may break under its own weight, resulting in a more dramatic decrease of the slab-pull force and favoring the onset of collision.

5. Discussion: Comparison With Previous Models and Natural System

[60] Analytical and numerical models based on buoyancy equilibrium calculations show that hundreds of km of continental lithosphere may subduct into the mantle [*Cloos*, 1993; *Ranalli*, 2000; *Ranalli et al.*, 2000]. Our experiments confirm these predictions but underline that a correct estimation of the possible amount of continental subduction should take into account the possibility for the slab to deform at depth, which requires a more complicated study than a simple buoyancy analysis. In fact, we observe that under the action of an external push related to the ridge or to plate reorganization, the continent can subduct into the mantle even if the subduction system is neutrally buoyant.

[61] *Funiciello et al.* [2001] show laboratory experiments of continental subduction following oceanic subduction with similar materials than those used here. In these experiments, the lithosphere/slab system is constituted by a thin viscous silicone sheet and the strength at the subduction fault is supposed to be low as the system does not include an upper plate. *Funiciello et al.* [2001] experiments are characterized by a low F_2 dimensionless parameter, since the velocity of convergence is high, and by a large F_1, since the brittle layer is not present. Because of the low F_2 parameter, the slab does not deform significantly during subduction. *Funiciello et al.*'s [2001] experiments show that a large amount of continental material can subduct if an external push is applied to the trailing edge of the plate. Comparison with our experiments underlines that the role of the resistance of the subduction fault is fundamental in generating the appropriate necessary conditions for collision.

[62] *Chemenda et al.* [1995, 1996, 2000] and *Pysklywec et al.* [2000] present models that reproduce a continental subduction. *Chemenda et al.* [1995, 1996, 2000] build up laboratory experiments that assume a plastic rheology for the lithosphere/slab system, while *Pysklywec et al.* [2000] use finite element calculations to study the subduction of a viscoplastic continental lithosphere underlain by a viscous mantle. Their initial boundary conditions, however, are similar. In both sets of experiments, the two continental plates are initially in contact, separated by a weak zone that absorbs the imposed shortening. Both of these sets of experiments differ from the experiments presented here, especially because their rheological profile (a weak lower crust in *Chemenda et al.*'s [1995, 1996, 2000] experiments, a continental crust much weaker than the mantle in *Pysklywec et al.*'s [2000] calculations) facilitates the delamination of the upper crust from the lithospheric mantle, that can readily subduct into the upper mantle.

[63] In *Pysklywec et al.*'s [2000] experiments, the continental crust is entirely accreted above the mantle fault and does not enter at depth. Then, the mantle thrust fault results in the formation of a dense negatively buoyant mantle slab that sinks into the convective mantle. It is interesting to observe that *Pysklywec et al.* [2000] obtain for some of their numerical experiments the formation of viscous drips and/or break-off of the subducted mantle. The shape and evolution of these viscous drips are similar to what occurs in our experiments. We calculated the F_1 and F_2 dimensionless numbers of these numerical experiments and placed the corresponding points in Figure 6b. F_1 and F_2 parameters give also a good description of the behavior of these numerical experiments: Viscous drips form in experiments characterized by high values of F_2, and both viscous drip and slab break-off occurs for high F_1 and F_2 experiments. On the contrary, the slab preserves its continuity when F_2 is small. The critical F_2 value over which viscous drips form, however, is larger in *Pysklywec et al.*'s [2000] calculations with respect to our experiments (Figure 6). This discrepancy may result from the different initial boundary conditions (for instance, the 10 mm large weak zone without sand that is initially present in our experiments at the future active margin facilitates the rapid formation of a viscous drip), or from the different asthenosphere viscosity (the asthenosphere is relatively more viscous in *Pysklywec et al.*'s [2000] calculations, which may delay the formation of the drip).

[64] *Chemenda et al.*'s [1995, 1996, 2000] experiments show that a large amount (200–300 km) of subduction of continental lithosphere can indeed occur, if the continental crust delaminates from the lithospheric mantle. They also show that continental slab can break off. However, these experiments cannot be directly compared with our experiments due to the different rheological set up of the model.

[65] The application of our experimental results to natural system is of course limited by the simplifications introduced in our experimental setup and by the elusive knowledge of the dynamics and rheology of subducted lithosphere. However, this study first shows the behavior of convergent margin during continental subduction after the closure of oceanic basin. We find that continental subduction cannot be used as a synonymous of collision. The two processes are different since a continent should subduct at large depths under the pull of the previously subducted ocean, before compressional structures develop near the surface. This could be the case in the northern Apennine, where foredeep analysis reveals that the slab-pull force remained active during continental subduction [*Royden*, 1993] and where more than 200–300 km of continent entered into the trench, pulled by the previously subducted oceanic lithosphere [*Faccenna et al.*, 2001; *Ranalli*, 2000; *Ranalli et al.*, 2000].

[66] We also find that the deep deformation of the oceanic portion of the slab can be easily obtained in laboratory, limiting the amount of "subductable" continental material. Stiff or short oceanic slabs, for example, may favor continental subduction since the subducted portion of ocean maintains its identity, structure and weight. Weak or long oceanic slab, conversely, may drip or break, drastically reducing the amount of subductable continental material. The formation of a viscous drip is possible if the slab can stretch sufficiently to detach from its upper part. Note that our models are built using a Newtonian viscous material. In nature, the viscous mantle acting as a non-Newtonian fluid, deformation is expected to be more localized and viscous drips may occur at faster rates and over a smaller length than in our experiments [*Conrad and Molnar*, 1997]. This

enlarges the possibilities to obtain the formation of viscous drips also for the case of a mantle in which circulation is limited by the presence of a 660-km-deep barrier. It is difficult to evidence the occurrence of such a mechanism in natural systems, though from tomographic images one can infer that slabs may deform viscously and leave parts of them to sink freely into the mantle [*van der Voo et al.*, 1999a]. In addition, it is rather well establish that slabs are submitted to in plane tension at intermediate depth, and that the reduction of the thickness of the seismogenic layer should correspond to the stretching and thinning of weak slabs [*Tao and O'Connell*, 1992].

[67] The other way to deform slabs is to break them entirely. Such a phenomenon may occur at a faster rate, and may abruptly separate the denser ocean from the lighter continent. Slab break-off mechanism has also been simulated numerically [*Pysklywec et al.*, 2000] and has been found to be a possible mechanism given the applied state of stress [*Wortel*, 1982; *van den Beukel*, 1992; *Wortel and Spakman*, 2000]. Slab break-off is often used to explain deformations that occurred for example in the Mediterranean, or in the New Hebrides [*Sorel et al.*, 1988; *Sébrier and Soler*, 1991; *Châtelain et al.*, 1992; *Wortel and Spakman*, 2000]. Its occurrence is expected to result in a rapid uplift of the overlying plate due to isostatic rebound. The rupture of the slab also favors the rapid onset of continental collision.

[68] Finally, our experiments suggest that continents may subduct for hundreds of kilometers into the mantle. The largest value we obtain corresponds to 450 km of continental subduction before collision starts. This number is in agreement with previous estimations and explains the observation of UHP rocks buried at depths larger than 25–30 kbar. However, this number should be considered as a lower bound as we perform our model in the less favorable conditions for continental subduction. We do not explore the possibility that lower crustal material is eclogitized, which drastically increases its density. We also do not consider the possibility to off scrape the crustal light material from the dense mantle. This mechanism permits the long-lasting subduction of the delaminated dense portion of the mantle and may explain the large amounts of Indian continent subducted beneath Asia.

6. Conclusion

[69] We explore the dynamics of continental subduction using laboratory experiments. We test the influence of parameters that we consider important in the evolution from subduction to continental collision: the total length of the subducting oceanic plate, the depth of the convecting mantle, and the lithosphere buoyancy. They play a role in equilibrating the total pull that can be exerted by the subducted slab. We show that the amount of continental subduction also depends on the strength of the slab, because the slab may deform during subduction, which may result in a decrease of the slab-pull force that drives the continental subduction. We define two dimensionless numbers F_1 and F_2 that characterize the possibility for the slab to deform during subduction. F_1 takes into account the total strength of the slab and characterizes the possibility for the slab to break, while F_2 marks the development of viscous dripping during subduction.

[70] The results of our experiments encompass many possible slab deformation modes and allow description of the collisional process from a dynamically consistent point of view. We show that continental subduction and collision are two different processes. Thus their use as synonymous terms should be avoided. A continent can subduct when pulled by a subducted portion of oceanic plate, with negligible surface shortening outside the trench. We observe that the amount of continent that can enter the trench is ultimately controlled by the buoyancy of the system. Collision occurs, in fact, when the subducting system becomes significantly positively buoyant. Only at that time, the trench locks and a thrust and fold belt accommodates the superficial shortening between both continental plates.

[71] **Acknowledgments.** V. Regard's modeling is part of his Ph.D. thesis collaborative project between the CEREGE (UMR-CNRS 6635) and the Laboratory Experimental Tectonics (University Roma Tre) supported by the French Research Ministry (Action spécifique, Cotutelle de thèse) and the "Galilée" project (Ministère des Affaires Etrangères). This study was developed in the framework of a wide cooperative French-Iranian project, supervised by D. Hatzfeld and M. G. Ashtiany. A portion of the program was set apart for studying the "modeling of young collision process", research funding being provided by the program Intérieur de la Terre (INSU-CNRS). We thank R. Pysklywec, S. Zhong, and M. Gerbault for helpful comments on the manuscript.

References

Austrheim, H., Eclogitization of lower crustal granulites by fluid migration through shear zones, *Earth Planet. Sci. Lett.*, *81*, 221–232, 1987.

Austrheim, H., Eclogitization of the deep crust in continent collision zones, *C. R. Acad. Sci., Ser II*, *319*, 761–774, 1994.

Becker, T. W., C. Faccenna, and R. J. O'Connel, The development of slabs in the upper mantle: insights from numerical and laboratory experiments, *J. Geophys Res.*, *104*, 15,207–15,227, 1999.

Bina, C. R., Phase transition buoyancy contributions to stresses in subducting lithosphere, *Geophys. Res. Lett.*, *23*, 3563–3566, 1996.

Bina, C. R., Patterns of deep seismicity reflect buoyancy stresses due to phase transitions, *Geophys. Res. Lett.*, *24*, 3301–3304, 1997.

Brace, W. F., and D. L. Kohlstedt, Limits on lithospheric stress imposed by laboratory experiments, *J. Geophys. Res.*, *85*, 6248–6252, 1980.

Buck, W. R., and M. N. Toksöz, Thermal effects of continental collisions: Thickening of a variable viscosity lithosphere, *Tectonophysics*, *100*, 53–69, 1983.

Byerlee, J., Friction of rocks, *Pure Appl. Geophys.*, *116*, 615–626, 1978.

Caby, R., Precambrian coesite from northern Mali: First record and implications for plate tectonics in the trans-Sahara segment of the Pan-African belt, *Eur. J. Mineral.*, *6*, 235–244, 1994.

Châtelain, J.-L., P. Molnar, R. Prévot, and B. Isacks, Detachment of part of the downgoing slab and uplift of the new Hebrides (Vanuatu) islands, *Geophys. Res. Lett.*, *19*, 1507–1510, 1992.

Chemenda, A. I., M. Mattauer, J. Malavieille, and A. N. Bokun, A mechanism for syn-collisional deep rock exhumation and associated normal faulting: results from physical modelling, *Earth Planet. Sci. Lett.*, *132*, 225–232, 1995.

Chemenda, A. I., M. Mattauer, and A. N. Bokun, Continental subduction and a mechanism for exhumation of high pressure metamorphic rocks: New modelling and field data from Oman, *Earth Planet. Sci. Lett.*, *143*, 173–182, 1996.

Chemenda, A. I., J.-P. Burg, and M. Mattauer, Evolutionary model of the Himalaya-Tibet system: Geopoem; based on new modelling, geological and geophysical data, *Earth Planet. Sci. Lett.*, *174*, 397–409, 2000.

Chopin, C., Coesite and pure pyrope in high-grade blueshists of the western Alps: A first record and some consequences, *Contrib. Mineral. Petrol.*, *86*, 253–274, 1984.

Cloos, M., Lithospheric buoyancy and collisional orogenesis: Subduction of oceanic plateaus, continental margins, island arcs, spreading ridges and seamounts, *Geol. Soc. Am. Bull.*, *105*, 715–737, 1993.

Conrad, C. P., and B. H. Hager, Effects of plate bending and fault strength at subduction zones on plate dynamics, *J. Geophys. Res.*, *104*, 17,551–17,571, 1999.

Conrad, C. P., and P. Molnar, The growth of Rayleigh-Taylor type instabilities in the lithiosphere for various rheological and density structures, *Geophys. J. Int.*, *129*, 95–112, 1997.

Davies, G. F., and M. A. Richards, Mantle convection, *J. Geol.*, *100*, 151–206, 1992.
Davies, J. H., and F. von Blanckenburg, Slab break-off: a model of lithosphere detachment and its test in the magmatism and deformation of collisional orogens, *Earth Planet. Sci. Lett.*, *129*, 85–102, 1995.
Davis, G. F., Mechanics of subducted lithosphere, *J. Geophys. Res.*, *85*, 6304–6318, 1980.
Davy, P., and P. R. Cobbold, Indentation tectonics in nature and experiment. 1. Experiments scaled for gravity, *Bull. Geol. Inst. Univ. Uppsala*, *14*, 129–141, 1988.
Davy, P., and P. R. Cobbold, Experiments on shortening of a 4-layer model, *Tectonophysics*, *188*, 1–25, 1991.
Dewey, J. F., P. D. Ryan, and T. B. Andersen, Orogenic uplift and collapse, crustal thickness, fabrics and metamorphic phase changes: The role of eclogites, in *Magmatic Processes and Plate Tectonics*, edited by H. M. Prichard et al., *Geol. Soc. Spec. Publ.*, *76*, 325–343, 1993.
England, P., and G. A. Houseman, Extension during continental convergence, with application to the Tibetan Plateau, *J. Geophys. Res.*, *94*, 17,561–17,579, 1989.
Ernst, W. G., and J. G. Liou, Overview of UHP metamorphism and tectonics in well-studied collisional orogens, in *Ultra-High Pressure Metamorphism and Geodynamics in Collision-Type Orogenic Belts*, edited by W. G. Ernst and J. G. Liou, pp. 3–19, *Geol. Soc. of Am.*, Boulder, Colo., 2000.
Faccenna, C., P. Davy, J.-P. Brun, R. Funiciello, D. Giardini, M. Mattei, and T. Nalpas, The dynamics of back-arc extension: An experimental approach to the opening of the Tyrrhenian Sea, *Geophys. J. Int.*, *126*, 781–795, 1996.
Faccenna, C., D. Giardini, P. Davy, and A. Argentieri, Initiation of subduction at Atlantic-type margins: Insights from laboratory experiments, *J. Geophys. Res.*, *104*, 2749–2766, 1999.
Faccenna, C., T. W. Becker, F. P. Lucente, L. Jolivet, and F. Rossetti, History of subduction and back-arc extension in the central Mediterranean, *Geophys. J. Int.*, *145*, 809–820, 2001.
Forsyth, D., and S. Uyeda, On the relative importance of the driving forces of plate motion, *Geophys. J. R. Astron. Soc.*, *43*, 163–200, 1975.
Funiciello, F., C. Faccenna, D. Giardini, and K. Regenauer-Lieb, Dynamics of advancing slabs: Insight from laboratory and numerical experiments, paper presented at 26th General Assembly, Geophys. Soc., Nice, France, 2001.
Griffiths, R. W., R. I. Hackney, and R. D. van der Hilst, A laboratory investigation of effects of trench migration on the decent of subducted slabs, *Earth Planet. Sci. Lett.*, *133*, 1–17, 1995.
Guillou-Frottier, L., J. Buttles, and P. Olson, Laboratory experiments on the structure of subducted lithosphere, *Earth Planet. Sci. Lett.*, *133*, 19–34, 1995.
Gurnis, M., and B. H. Hager, Controls on the structure of subducted slabs, *Nature*, *335*, 317–321, 1988.
Hager, B. H., Subducted slab and the geoid: Constraints on mantle rheology and flow, *J. Geophys. Res.*, *89*, 6003–6015, 1984.
Hager, B. H., and R. J. O'Connell, A simple global model of plate dynamics and mantle convection, *J. Geophys. Res.*, *86*, 4843–4867, 1981.
Houseman, G. A., and D. Gubbins, Deformation of subducted oceanic lithosphere, *Geophys. J. Int.*, *131*, 535–551, 1997.
Houseman, G. A., and P. Molnar, Gravitational (Rayleigh-Taylor) instability of a layer with non-linear viscosity and convergence thinning of continental lithosphere, *Geophys. J. Int.*, *128*, 125–150, 1997.
Houseman, G. A., D. P. McKenzie, and P. Molnar, Convective instability of a thickened boundary layer and its relevance for the thermal evolution of continental convergent belts, *J. Geophys. Res.*, *86*, 6115–6132, 1981.
Isacks, B., and P. Molnar, Distribution of stresses in the descending lithosphere from a global survey of focal mechanisms solutions of mantle earthquake, *Rev. Geophys.*, *9*, 175–193, 1971.
Karason, H., and R. D. van der Hilst, Constraints on mantle convection from seismic tomography, in *The History and Dynamics of Global Plate Motions*, *Geophys. Monogr. Ser.*, vol. 121, edited by M. A. Richards, R. G. Gordon, and R. D. van der Hilst, pp. 277–288, AGU, Washington, D. C., 2000.
Katayama, I., C. D. Parkinson, K. Okamoto, Y. Nakajima, and S. Maruyama, Supersilisic clinopyroxene and silica exsolution in UHPM eclogite and pelitic gneiss from the Kokchetav massif, Kazakhstan, *Am. Mineral.*, *85*(10), 1368–1374, 2000.
Kincaid, C., and P. Olson, An experimental study of subduction and slab migration, *J. Geophys. Res.*, *92*, 13,832–13,840, 1987.
Lambeck, K., P. Johnston, and M. Nakada, Holocene glacial rebound and sea-level change in NW Europe, *Geophys. J. Int.*, *103*, 451–468, 1990.
Lenardic, A., and W. M. Kaula, More thoughts on convergent crustal plateau formation and mantle dynamics with regard to Tibet, *J. Geophys. Res.*, *100*, 15,193–15,203, 1995.
Le Pichon, X., M. Fournier, and L. Jolivet, Kinematics, topography, shortening and extrusion in the India-Eurasia collision, *Tectonics*, *11*, 1085–1098, 1992.
Le Pichon, X., P. Henry, and B. Goffé, Uplift of Tibet: From eclogites to granulites-implications for the Andean Plateau and the Variscan Belt, *Tectonophysics*, *273*, 57–76, 1997.
Liou, J. G., B. R. Hacker, and R. Y. Zhang, Ultrahigh-pressure (UHP) metamorphism in the forbidden zone, *Science*, *287*, 1215–1216, 2000.
Lithgow-Bertelloni, C., and M. A. Richards, The dynamics of Cenozoic and Mesozoic plate motions, *Rev. Geophys.*, *36*, 27–78, 1998.
Mandl, G., L. N. J. De Jong, and A. Maltha, Shear zones in granular material, *Rock Mech.*, *9*, 95–144, 1977.
Martinod, J., and P. Davy, Periodic instabilities during compression or extension of the lithosphere: 1. Deformation modes from an analytical perturbation method, *J. Geophys. Res.*, *97*, 1999–2014, 1992.
Martinod, J., and P. Davy, Periodic instabilities during compression or extension of the lithosphere: 2, Analogue experiments, *J. Geophys. Res.*, *99*, 12,057–12,069, 1994.
Marton, F., C. R. Bina, S. Stein, and D. C. Rubie, Effects of slab mineralogy on subduction rates, *Geophys. Res. Lett.*, *26*, 119–122, 1999.
Matte, P., M. Mattauer, J. M. Olivet, and D. A. Griot, Continental subductions beneath Tibet and the Himalayan orogeny: A review, *Terra Nova*, *9*, 264–270, 1997.
McKenzie, D. P., Speculations on the consequences and causes of plate motions, *Geophys. J. R. Astron. Soc.*, *18*, 1–32, 1969.
McKenzie, D. P., The initiation of trenches: A finite amplitude instability, in *Island Arcs Deep Sea Trenches and Back-Arc Basins*, *Maurice Ewing Ser.*, vol. 1, edited by M. Talwani and W. C. Pitman III, pp. 57–61, AGU, Washington, D. C., 1977.
Molnar, P., G. A. Houseman, and C. P. Conrad, Rayleigh-Taylor-type instability and convective thinning of mechanically thickened lithosphere: Effects of non-linear viscosity decreasing exponentially with depth and horizontal shortening of the layer, *Geophys. J. Int.*, *133*, 568–584, 1998.
Muller, S., and R. J. Phillips, On the initiation of subduction, *J. Geophys. Res.*, *96*, 651–665, 1991.
Neil, E. A., and G. A. Houseman, Rayleigh-Taylor instability of the upper mantle and its role in intraplate orogeny, *Geophys. J. Int.*, *138*, 89–107, 1999.
Parsons, B., and F. M. Richter, A relation between the driving force and geoid anomaly associated with mid-oceanic ridges, *Earth Planet. Sci. Lett.*, *51*, 445–450, 1980.
Patriat, P., and J. Achache, India-Eurasia collision chronology has implications for crustal shortening and driving mechanism of plates, *Nature*, *311*, 615–621, 1984.
Pubellier, M., and P. R. Cobbold, Analogue models for the transpressional docking of volcanic arcs in the western Pacific, *Tectonophysics*, *253*, 33–52, 1996.
Pysklywec, R. N., C. Beaumont, and P. Fullsack, Modeling the behaviour of the continental mantle lithosphere during plate convergence, *Geology*, *28*(7), 655–658, 2000.
Ranalli, G., Rheology and subduction of continental lithosphere, in *Crust Mantle Interactions, Proceedings of the International School of Earth and Planetary Sciences*, pp. 21–40, Int. Sch. of Earth and Planet. Sci., Siena, Italy, 2000.
Ranalli, G., and D. C. Murphy, Rheological stratification of the lithosphere, *Tectonophysics*, *132*, 281–296, 1987.
Ranalli, G., R. Pellegrini, and S. D'Affizi, Time dependance of negative buoyancy and the subduction of continental lithosphere, *J. Geodyn.*, *30*, 539–555, 2000.
Royden, L. H., Evolution of retreating subduction boundaries formed during continental collision, *Tectonics*, *12*, 629–638, 1993.
Schmeling, H., R. Monz, and D. C. Rubie, The influence of olivine metastability on the dynamics of subduction., *Earth Planet. Sci. Lett.*, *165*, 55–66, 1999.
Sébrier, M., and P. Soler, Tectonics and magmatism in the Peruvian Andes from late Oligocene time to Present, *Spec. Pap. Geol. Soc. Am.*, *265*, 259–277, 1991.
Shemenda, A. I., Horizontal lithosphere compression and subduction: Constraints provided by physical modelling, *J. Geophys. Res.*, *97*, 11,097–11,116, 1992.
Smith, D. C., Coesite in clinopyroxene in the Caledonides and its implication for geodynamics, *Nature*, *310*, 641–644, 1984.
Sorel, D., J. L. Mercier, B. Keraudren, and M. Cushing, Le rôle de la traction de la lithosphère subductée dans l'évolution géodynamique Plio-Pleistocène de l'arc égéen: Mouvement verticaux alternés et variations du régime tectonique, *C. R. Acad. Sci., Ser. II*, *307*, 1981–1986, 1988.
Spence, W., Slab pull and the seismotectonics of subducting lithosphere, *Rev. Geophys.*, *25*, 55–69, 1987.

Tao, W. C., and R. J. O. O'Connell, Ablative subduction: A two-sided alternative to the conventional subduction model, *J. Geophys. Res.*, *91*, 8877–8904, 1992.

Tichelaar, B. W., and L. J. Ruff, Depth of seismic coupling along subduction zones, *J. Geophys. Res.*, *98*, 2017–2037, 1993.

Turcotte, D. L., and G. Schubert, *Geodynamics: Applications of Continuum Physics to Geological Problems*, John Wiley, New York, 1982.

van den Beukel, J., Some thermo-mechanical aspects of the subduction of continental lithosphere, *Tectonics*, *11*, 316–329, 1992.

van der Voo, R., W. Spakman, and H. Bijwaard, Mesozoic subducted slabs under Siberia, *Nature*, *397*, 246–249, 1999a.

van der Voo, R., W. Spakman, and H. Bijwaard, Tethyan subducted slabs under India, *Earth Planet. Sci. Lett.*, *171*, 7–20, 1999b.

Vlaar, N. J., and M. J. R. Wortel, Lithospheric ageing, instabilities and subduction, *Tectonophysics*, *32*, 331–351, 1976.

Wain, A., New evidence for coesite in eclogites and gneiss: Defining an ultrahigh-pressure province in the Western Gneiss region of Norway, *Geology*, *25*, 927–930, 1997.

Weijermars, R., and H. Schmeling, Scaling of Newtonian and non Newtonian fluid dynamics without inertia for quantitative modelling of rock flow due to gravity (including the concept of rheological similarity), *Phys. Earth Planet. Inter.*, *43*, 316–330, 1986.

Wong A Ton, S. Y. M., and M. J. R. Wortel, Slab detachment in continental collision zones: An analysis of controlling parameters, *Geophys. Res. Lett.*, *24*, 2095–2098, 1997.

Wortel, R., Seismicity and rheology of subducted slabs, *Nature*, *296*, 553–556, 1982.

Wortel, M. J. R., and W. Spakman, Subduction and slab detachment in the Mediterranean-Carpathian region, *Science*, *290*, 1910–1917, 2000.

Yoshioka, S., and M. J. R. Wortel, Three-dimensional numerical modelling of detachment of subducted lithosphere, *J. Geophys. Res.*, *100*, 20,223–20,244, 1995.

Zhong, S., and M. Gurnis, Controls on trench topography from dynamic models of subducted slabs, *J. Geophys. Res.*, *99*, 15,683–15,695, 1994.

Zhou, H.-W., Observations on earthquake stress axes and seismic morphology of deep slabs, *Geophys. J. Int.*, *103*, 377–401, 1990.

O. Bellier and V. Regard, CEREGE, UMR CNRS 6635, Université Aix-Marseille III, Europôle de l'Arbois, F-13545 Aix-en-Provence cedex 4, France. (bellier@cerege.fr; regard@cerege.fr)

C. Faccenna, Dipartimiento di Scienze Geologiche, Università Roma tre, Largo S. L. Murialdo 1, I-00146, Rome, Italy. (faccenna@uniroma3.it)

J. Martinod, IRD-LMTG, 38 rue des 36 ponts, f-31400 Toulouse, France. (martinod@lmtg.ups-tlse.fr)

J.-C. Thomas, LGIT, UMR CNRS 5559, Université Joseph Fourier, BP 53, 38041 Grenoble cedex 9, France.